JOURNAL OF MATERIALS SCIENCE 15 (1980) 2455–2465

Analysis of flaws in high-strength carbon fibres from mesophase pitch

JANICE BREEDON JONES, JOHN B. BARR, ROBERT E. SMITH
Union Carbide Corporation, Carbon Products Division, Parma Technical Centre, Parma, Ohio 44130, USA

Defects in mesophase pitch-based carbon fibres were studied by using scanning electron microscopy and energy dispersive X-ray analysis. A novel fractography technique permitted routine recovery of the primary fracture surfaces of filaments tested in tension. The carbon fibres included experimental monofilaments spun on laboratory equipment and multifilaments spun as a continuous fibre on production-type equipment. Carbon monofilaments and multifilaments from clean mesophase pitches were stronger than similarly prepared fibres from contaminated pitches. Reduction in the levels of contamination allowed fibres to be processed at high heat-treatment temperatures without sacrificing tensile strength. Results from a Weibull analysis of the tensile strength of clean multifilaments as a function of test gauge length were consistent with microscopy observations that strength-limiting surface flaws were closely spaced along the filaments.

1. Introduction

The tensile strengths of carbon fibres are limited by a spectrum of defects which are distributed randomly along the fibre length. The probability of encountering a severe flaw becomes greater as the test length of the filament increases. The inverse dependence of tensile strength on gauge length has been reported for carbon fibres made from polyacrylonitrile (PAN) [1–4], rayon [5], and mesophase pitch [6] precursors. Numerous commercially available high modulus fibres from PAN-based carbon, boron, S–glass, and Kevlar have been shown to behave similarly [7].

The strength of pitch-based carbon fibres has been estimated at 7 GPa at 0.1 mm length by Weibull statistical analysis of strength data [6]. In like manner, Thorne [3] has estimated from loop tests at an effective gauge length of 0.1 mm intrinsic tensile strengths exceeding 6 GPa for PAN-based carbon fibres. By using a weakest link model, Diefendrof and Tokarsky [8] reported an estimated strength of 8 GPa for PAN-based carbon fibres at the very short gauge length of 0.02 mm.

Sources of failure of PAN-based carbon fibres have been identified as internal and surface flaws by scanning electron microscopy of the fracture surfaces of filaments broken in tension [4, 9, 10]. The sizes and distributions of internal flaws have been determined by Sharp *et al.* [11, 13] by using high-voltage electron microscopy. These investigators reported that inclusions appeared to become volatile at heat-treatment temperatures over 1800° C, leaving voids in the carbonized filaments. Microradiography and several microscopic methods were used by Jorro *et al.* [13] to examine voids and inclusions in coal-based carbon fibres. These authors pointed out that the nature of flaws in PAN-based carbon fibres has been studied extensively, but that little is known about defects in carbon fibres from coal and petroleum feedstocks.

The strength of PAN-based carbon fibres usually exhibits a carbonization temperature dependence. A heat-treatment temperature of approximately 1500° C produces maximum strength [1, 9, 12, 14]. The importance of impurities in determining this temperature–tensile strength pattern was established by Moreton and Watt [15]. These investigators found that fibres spun under clean room conditions from a filtered polymer solution

0022–2461/80/102455–11 $03.10/0

continued to increase in strength with increasing heat-treatment temperature in tests up to 2500° C.

In the present work, flaws causing failure of carbonized filaments prepared from mesophase pitch have been determined by examining with scanning electron microscopy the fracture surfaces of single filaments tested in tension. Mesophase pitches were spun on laboratory monofilament apparatus and on production-prototype multifilament equipment. Tensile strength distributions have been measured for multifilament fibres at various gauge lengths and the strength data analysed by using Weibull failure statistics. Tensile strengths of monofilaments and of multifilaments spun and processed on production-scale equipment have been shown to be higher when care is taken to avoid contamination of the pitch from which the filaments were made.

2. Experimental procedure

Fibres were spun from mesophase pitches which included some pitches prepared with special precautions to avoid contamination and others made under less stringent conditions of cleanliness. Fibres were spun either as monofilaments or as 1000- or 2000-filament yarns. A single-hole spinnerette, which has been described previously [16], was used to spin monofilaments from pitches prepared with laboratory-scale equipment. These monofilaments were rendered infusible by oxidation [16] and carbonized by heating in an inert atmosphere.

Multifilament yarns were prepared from production-size quantities of mesophase pitch, and production-prototype equipment was used for spinning and processing. After being made infusible, the multifilament fibres were carbonized at high temperatures.

Tensile strengths of single filaments were measured at gauge lengths of 20 and 3.2 mm by using test conditions that allowed recovery of the primary fracture surfaces needed for identifying critical flaws. A fractography technique has been developed that involves coating test filaments with a water-soluble stopcock grease to prevent fragmentation during tensile testing. The present method is simpler than the liquid bath methods used previously [1, 9] because conventional test equipment is used.

The conventional part of the procedure involves cementing the fibre with wax to a cardboard tensile tab and testing the filament with an Instron machine after cutting through both sides of the tab. The novel aspects of the test are shown in Fig. 1. One end of the tab is taped to a standard microscope slide, which is inserted into the upper grip of the test machine. The other end of the tab overhangs the end of the slide by approximately 5 mm to provide an area for the lower grip. The microscope slide provides a support surface for grease which surrounds the fibre and helps to prevent fragmentation. The grease, which is a key component in the current test, must have the proper viscosity. A very fluid grease will flow from the test sample, but a very viscous grease cannot be applied to the fibre without causing failure.

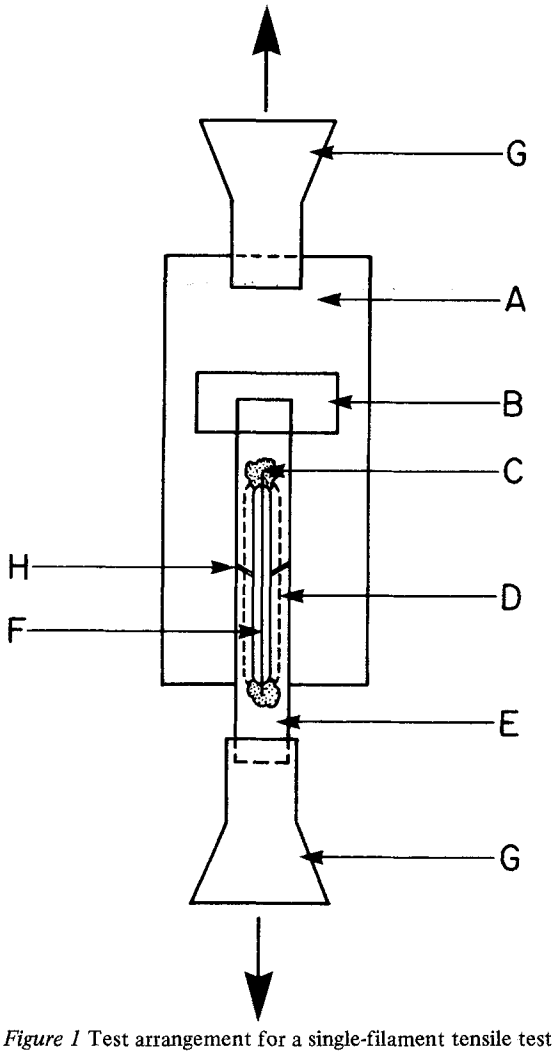

Figure 1 Test arrangement for a single-filament tensile test permitting the recovery of matching fracture surfaces. (A) glass microscope slide, (B) adhesive tape, (C) wax, (D) stopcock grease, (E) cardboard tab, (F) fibre, (G) grips, (H) cut through cardboard tab.

The grease must also be easy to remove with a solvent which will not attack the mounting wax on the tensile tab. A grease which fits these criteria is a blend of water-soluble greases, Nonaq (Fisher Scientific Company) and Phynal (Sargent–Welch), in the approximate proportion of two parts Phynal to one part Nonaq. The force necessary to pull the tensile tabs through the grease during a test has been found to be negligible compared with the force necessary to break the fibre. These modifications to the conventional fibre tensile test provide a simple method for measuring the fibre strength and recovering fracture surfaces for identifying flaws responsible for failure.

After the fibre has broken, the glass slide with the tensile tab still tacked to it by the grease is carefully removed from the test machine, and the filament break is inspected microscopically. Only fibres which clearly failed within the gauge section are retained for further study. The slide with attached tabs and fibre is immersed in a petri dish of distilled water to dissolve most of the grease. The fibre is removed from the water and allowed to dry in air, the cardboard tab is trimmed off, and the fibre is then cemented with silver paint to a specimen mount for scanning electron microscopy. The mounted fibre is soaked in detergent and water to remove any remaining grease.

This procedure routinely allows recovery of matching fracture surfaces in approximately 75% of the breaks within the fibre gauge section. The greatest source of failure to obtain matching surfaces is loss during handling of one of the two fibre fragments. Fragmentation into several pieces in the grease medium occurs in only a few per cent of the test specimens.

Fibre fracture surfaces were examined with a JEM-100C electron microscope in the secondary electron scanning mode. Elemental analysis was performed with a Kevex energy dispersive X-ray analysis unit attached to the microscope. Cross-sectional areas of the fracture surfaces were determined by comparison with latex calibration spheres.

Fibres for Weibull analysis were broken by using conventional testing procedures. The cross-sectional areas were determined from the average of maximum and minimum diameters obtained by scanning along the filaments with an image shearing microscope.

3. Results

3.1. Monofilaments

3.1.1. Strengths

Table I presents tensile strengths determined by fractography testing, at gauge lengths of 20 mm and 3.2 mm, of carbon fibres spun as monofilaments. The weaker fibre, A, which exhibited a single-filament tensile strength at 20 mm gauge length of only 1.2 GPa, was made without special precautions for cleanliness. Fibres from pitches prepared with care to minimize contamination (Fibres B and C) had tensile strength averages of 2.4 to 2.6 GPa.

The average tensile strengths for the mono-

TABLE I Single filament fractography tensile strengths of monofilament and multifilament samples

Sample		Heat treatment temperature (° C)	20 mm long gauge (LG) tensile strength		3.2 mm short gauge (SG) tensile strength		Number of tests	
			Average (GPa)	Standard deviation (GPa)	Average (GPa)	Standard deviation (GPa)	LG	SG
Monofilaments								
A (contaminated)		1750	1.2	0.43	2.1	0.32	7	9
B (clean)		1700	2.4	0.66	3.0	0.57	12	10
C (clean)		1750	2.6	0.64	2.9	0.85	10	11
Multifilaments								
	1	1700	1.7	0.28	1.9	0.28	16	20
D (contaminated)	2	2100	1.9	0.28	2.1	0.33	30	19
	3	2500	1.5	0.32	1.9	0.17	21	13
	1	2100	2.7	0.37	3.0	0.33	15	8
E (clean)	2	2500	2.6	0.30	3.2	0.27	12	8
	3	2800	2.8	0.49	3.3	0.41	10	10

TABLE II Distribution of flaws in carbonized monofilaments

Sample		Average strength (GPa)	Defects (%)				
			Mineral particles	Ferrous particles	Unknown particles	Gas bubbles	Undetected defects
A (contaminated)	LG	1.2		100			
	SG	2.1		56	11		33
B (clean)	LG	2.4	8	42	17	8	25
	SG	3.0	10	20		20	50
C (clean)	LG	2.6	10	50	30		10
	SG	2.9	91*	27*	9		

* Three defects showed both mineral and stainless steel elements.

filaments were higher for 3.2 mm than for 20 mm gauge length, a result which is usually indicative of a flaw-dependent failure mode [6]. The large scatter in strength is typical of single-filament testing of carbon fibres.

3.1.2. Microscopy

The fracture surfaces of the monofilaments contained several types of flaws of varying severity (Table II). The general classifications were mineral particles, ferrous particles, unknown particles, gas bubbles, and undetected defects. Scanning electron micrographs of monofilament fracture surfaces are shown in Figs. 2 to 5. The fracture surfaces showed an asymmetrical combination of radial and circumferential elements with a fine-grained structure at the outer edge. The tensile strength listed with each micrograph is the strength of the filament shown, but a wide variation in strength was found among fibres with similar defects.

3.1.2.1. Mineral particles. One class of common particle flaws consisted of inorganic particles which usually contained silicon and often contained other elements, such as aluminium, calcium, and magnesium. The major axes of the particles ranged in size from less than one micron to several microns. Jorro *et al.* [13] suggested a clay mineral origin for particles with similar elemental composition in inclusions found at the broken ends of carbon filaments from coal extract. After heat treatment of the present fibres, cavities had developed around most of the particles; however, a few particles were still tightly embedded in the carbon. The cavities may originate from the vapourization of particles [11] or from the reaction of particles with the surrounding carbon. Particles were usually near the edge of the fracture surface and were associated with a swelling that distorted the filament cross-section. A typical mineral particle at the edge of the fracture surface of a carbon filament is shown in Fig. 2.

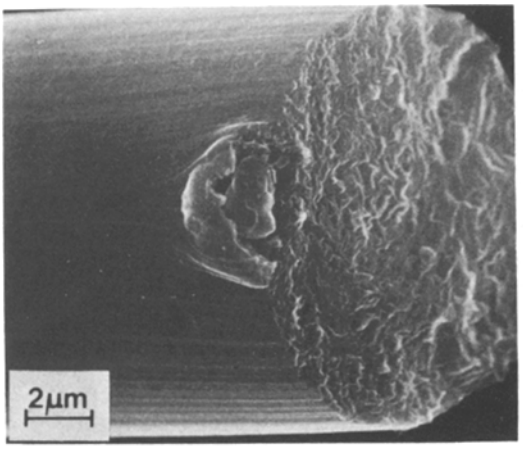

Figure 2 Scanning electron micrograph of a particle containing silicon and aluminium on the outer surface of a carbon monofilament. Tensile strength, 1.5 GPa.

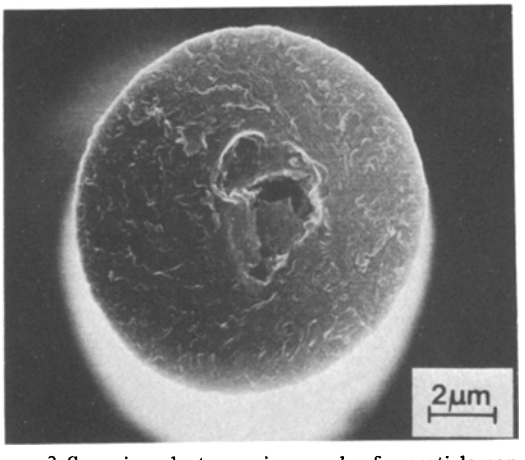

Figure 3 Scanning electron micrograph of a particle containing iron, chromium, and nickel in the interior of a carbon monofilament. Tensile strength, 2.4 GPa.

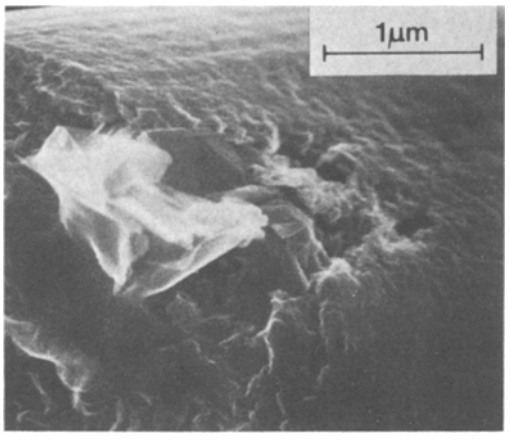

Figure 4 Scanning electron micrograph showing pitting surrounding an iron-containing particle on the outer surface of a carbon monofilament. Tensile strength, 1.8 GPa.

3.1.2.2. Ferrous particles. Particles containing iron were also encountered frequently on monofilament fracture surfaces. The iron was often in combination with chromium and nickel or, occasionally, with silicon. Iron particles in the interior of the filaments were in cavities, and those on the filament surfaces were surrounded by a region with a high concentration of shallow pits. Filaments with internal flaws (Fig. 3) were generally stronger than filaments with flaws of the same size at the edge of the fracture surface. The holes and pits around ferrous particles were probably caused by reaction between the particle and the surrounding carbon. Ferrous surface particles often had a shape that resembled a crumpled sheet (Fig. 4). The ferrous inclusions were in the same submicron to two-micron size range as the mineral inclusions. The iron, chromium and nickel particles came from stainless steel processing equipment.

3.1.2.3. Miscellaneous defects. A few voids were found with morphologies similar to those of cavities formed by particles, but particles could not be detected in them visually or by X-ray elemental analysis. These defects have been classified in Table II as unknown particles. Gas bubbles were rare in these carbon filaments, but a few elongated internal bubbles were found in fibre B.

3.1.2.4. Undetected defects. The defect causing failure of some of the strongest filaments could not be detected by examining the matching fracture surfaces (Fig. 5). This difficulty was frequently encountered in filaments with strengths above 2.8 GPa since the SEM technique is not suitable for detecting submicron-sized flaws or structural irregularities.

3.2. Multifilaments

3.2.1. Strengths

Multifilament carbon fibres from fibre E, prepared under conditions to minimize contamination, were stronger at each processing temperature and test gauge length than the more contaminated filaments from fibre D (Table I). Fig. 6 shows the effect of heat-treatment temperature on tensile strength for fibres D and E. The strength of fibre D reached a maximum (of 1.9 GPa) and then decreased with heating to higher temperatures. This behaviour was also shown by fibre F (Fig. 7), a contaminated fibre similar to fibre D. On the other hand, the tensile strength of the clean fibre, fibre E, was nearly independent of heat-treatment temperature

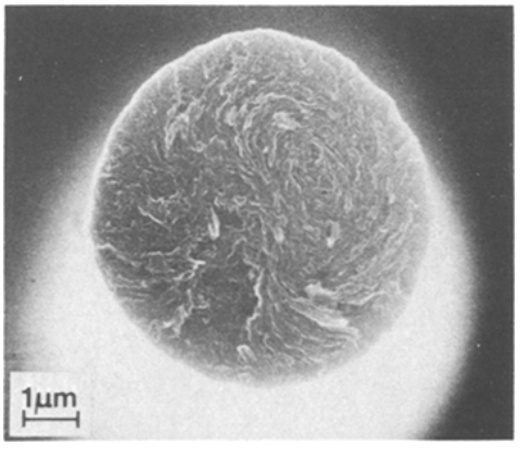

Figure 5 Scanning electron micrograph of the fracture surface of a monofilament which failed at an undetected defect. Tensile strength, 3.8 GPa.

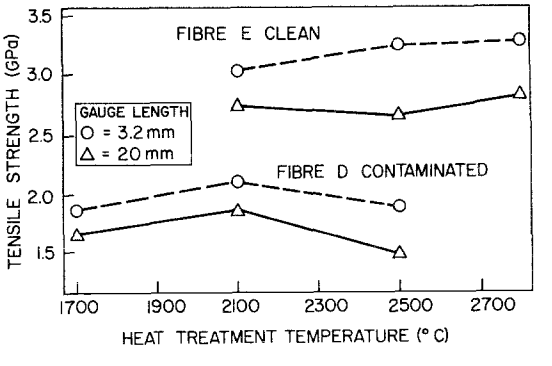

Figure 6 The effect of heat-treatment temperature on the long- and short-gauge tensile strengths of contaminated fibre D and clean fibre E.

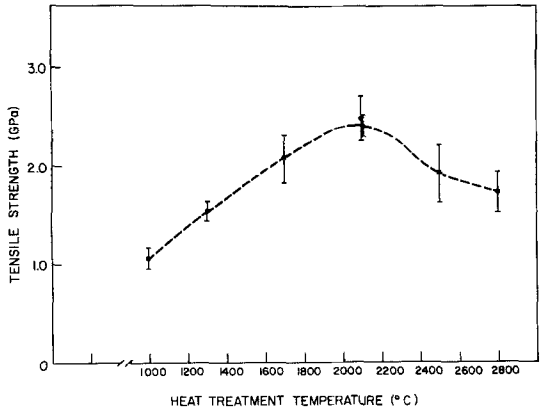

Figure 7 The effect of heat-treatment temperature on the tensile strength at 20 mm gauge length of contaminated fibre F. The bars show one standard deviation.

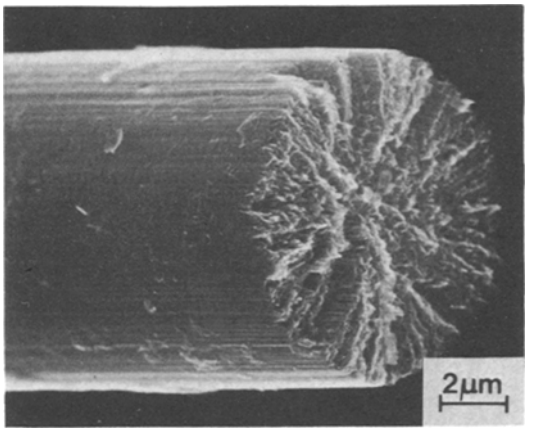

Figure 8 Scanning electron micrograph showing the rough fracture surface of a multifilament pitch-based carbon fibre heat treated at 2500° C. Tensile strength, 3.1 GPa.

over a wide range of carbonization temperatures. The strength values had the scatter typical of single filament testing; however, the trends have been verified by testing carbonized multifilament yarns as epoxy-impregnated strands.

3.2.2. Microscopy

The carbonized multifilament fibres had a wider variety of strength-limiting flaws (Table III) than the monofilament samples. The multifilament classifications were particles, surface pits, small surface holes, miscellaneous defects, and undetected defects.

Fig. 8 illustrates some aspects of the general structure of multifilament fibres. The arrangement of crystallites had an overall radial symmetry; a transverse view of this symmetry is visible in the undistorted portion of the fibre in Fig. 11. The radial orientation has been confirmed by numerous observations with optical microscopy. The fracture surface was "pulled-out" in appearance, with a tendency towards longitudinal cleavage that increased at higher carbonization temperatures. The interior longitudinal surfaces thus revealed had a fibrillar texture similar to that on the outside of the fibre.

3.2.2.1. Mineral particles. Particles in the carbon fibres spun as multifilaments closely resembled the mineral inclusions found on the fracture surfaces of carbon filaments from monofilament spinning. Similarities included elemental composition, size

TABLE III Distribution of flaws in carbonized multifilaments

Sample			Average strength (GPa)	Defects (%)				
				Particle flaws	Small smooth surface holes	Surface pits	Misc. defects	Undetected defects
D (contaminated)	1	LG	1.7	58	15		27	
		SG	1.9	60	30	5	5	
	2	LG	1.9	47	27	3	23	
		SG	2.1	53	32		15	
	3	LG	1.5	95	5			
		SG	1.9	85	15			
E (clean)	1	LG	2.7	7		13	7	73
		SG	3.0	13		13	13	61
	2	LG	2.6	50		17	8	25
		SG	3.2	25		38	12	25
	3	LG	2.8	40			40	20
		SG	3.3	10		30	30	30

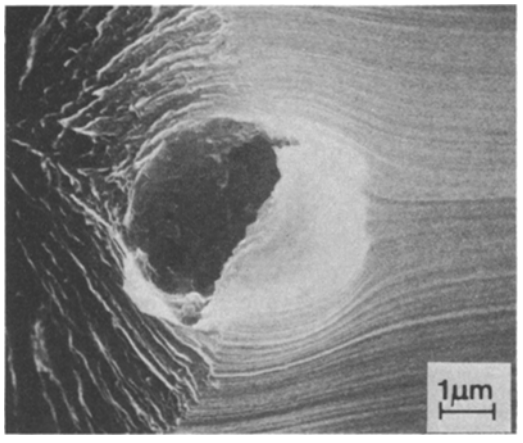

Figure 9 Scanning electron micrograph of a flaw caused by a particle containing silicon, aluminium and calcium in a multifilament carbonized at 2100° C. Tensile strength, 1.2 GPa.

range, preferred location near the filament surface, and association with holes. However, the holes were more often empty or nearly empty in multifilament fibres, particularly after the fibres were subjected to processing temperatures higher than 1700° C. Many holes had morphologies that placed them in the "particle" category, but gave no X-ray signals from foreign elements. The stainless steel particles so common in the monofilaments were absent from fracture surfaces of the multifilament samples.

Fig. 9 shows a typical particle flaw in a fractured filament from fibre D heat treated at 2100° C. The flaw contained silicon, aluminium, and calcium. The bent lines in the carbon structure suggest a flow pattern that was established during spinning. Most particles had partially or completely disappeared during the 1700° C and 2100° C heat treatments, leaving voids with average sizes of 1.5 μm. The average diameters of the holes increased to over 2.5 μm for filaments heat treated at 2500° C.

The evolution of the flaws with increasing heat treatment was examined for fibre F, a contaminated fibre which failed at mineral particles. Fig. 10a shows an irregular particle, containing aluminium and silicon, in the fracture surface of a filament which had been made infusible but which had not been carbonized. Little separation was visible between the particle and the surrounding material. Examination of filaments after the first stages of carbonization showed little change in the appearance of the particle flaws. Heat treatment at

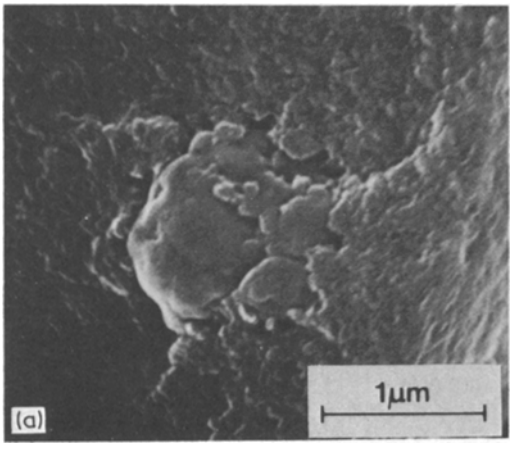

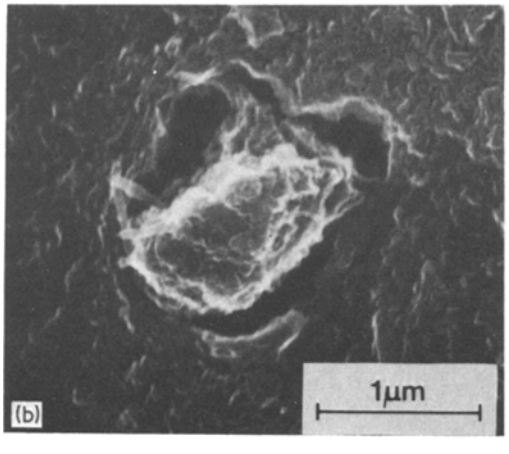

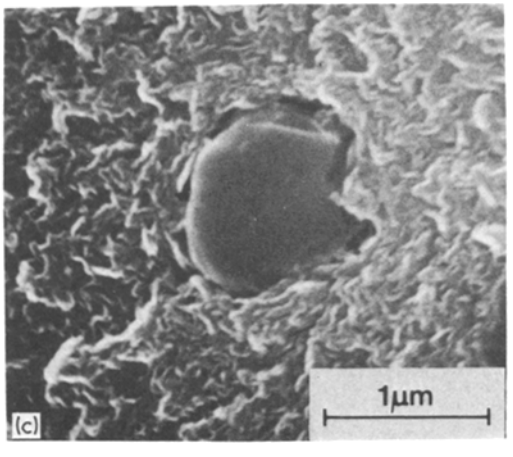

Figure 10 Scanning electron micrographs of particle flaws containing silicon and aluminum in contaminated fibre F. (a) Typical particle in a filament which had been made infusible. (b) Particle in a void after carbonization at 1700° C. Tensile strength, 2.1 GPa. (c) Particle which survived heat treatment at 2100° C. Tensile strength, 2.7 GPa.

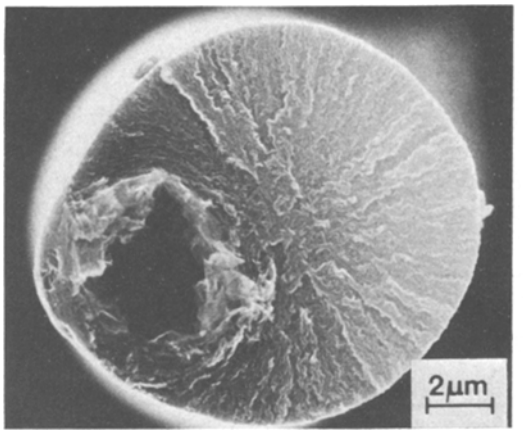

Figure 11 Scanning electron micrograph of a particle flaw in contaminated fibre D after heat treatment at 2500° C. No foreign elements were detected with the X-ray analyser. Tensile strength, 1.3 GPa.

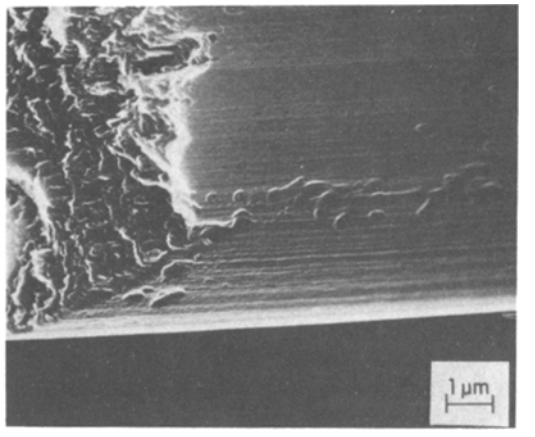

Figure 12 Scanning electron micrograph of surface pits in a clean multifilament. Tensile strength, 2.5 GPa.

1700° C produced some holes, some voids that contained particles of reduced size (Fig. 10b), and some particles which were almost unchanged in appearance. A few particles also survived heat treatment at higher temperatures (Fig. 10c). They often had smoother surfaces, suggesting that they had undergone partial melting. The variability in particle survival probably reflects differences in composition among the particles, though holes could have been the result of particles which had fallen out on fracture.

Both fibres D and F exhibited enlarged holes after heat treatment at high temperatures. An example of such a hole from fibre D is shown in Fig. 11. The enlargement of these holes was probably responsible for the decrease in strength of contaminated fibres after high heat-treatment temperatures.

The sheet-like linings of the hole in Fig. 11 and of one other hole in fibre D protruded far enough from the fracture surface to permit electron beam diffraction. Many microbeam diffraction patterns were taken with a beam less than 1000 Å in diameter from the material around the two holes, and only one pattern showed even a slight doubling of the (1 0) ring. This evidence indicates the existence of insignificant amounts of graphite formation around these two holes. In contrast, Sharp and Burnay [17] found extensive graphitization around flaws in PAN-based fibres heated to 2600° C, but the composition of the particles that had formed the holes was not known.

3.2.2.2. Surface pitting. Filament failure at surface pits was encountered most frequently in fibre E (clean). The filament in Fig. 12 is a typical example of closely-spaced surface pitting.

3.2.2.3. Small surface holes. Broken filament ends of fibre D often contained surface holes with smooth inner surfaces and diameters of approximately 1 μm (Fig. 13). Although they gave no X-ray traces from foreign elements, the voids were probably caused by particles rather than by gas bubbles, since they were not elongated and were not found in clean filaments.

3.2.2.4. Miscellaneous defects. Uncommon miscellaneous defects included an assortment of flaws

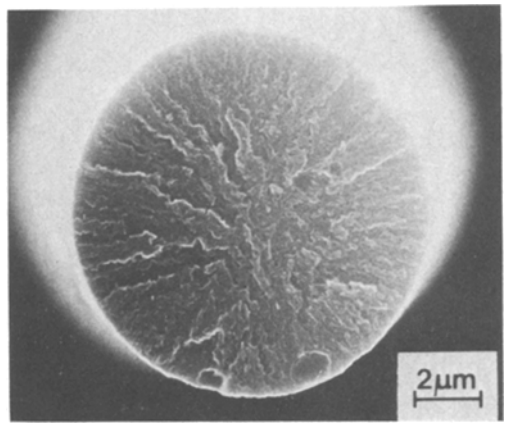

Figure 13 Scanning electron micrograph of a multifilament with small smooth surface holes probably caused by particles of unknown composition. Tensile strength, 2.0 GPa.

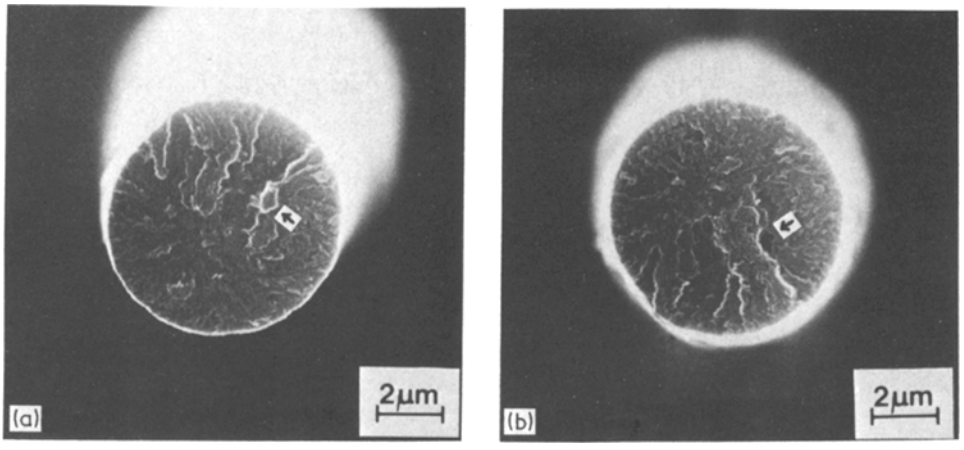

Figure 14 Scanning electron micrographs of matching fracture surfaces containing a local inhomogeneity which might have initiated fracture. Tensile strength, 3.1 GPa.

from mechanical damage or interfilament sticking. Occasionally, a fibre with pronounced radial structure developed a longitudinal crack that enlarged during carbonization, giving a "missing wedge" appearance [16].

3.2.2.5. Undetected defects. Defects causing the fracture of some filaments in fibre E were too small or too poorly defined to be recognizable in the electron micrographs. Because the roughness of the fracture surfaces of pitch-based carbon fibres does not change as distance from the origin of fracture increases, no clues about the locations of undetected critical flaws were available. Either surface or bulk defects might have caused failure. Small surface defects (for example, surface pitting) can be very difficult to detect. One possible bulk defect is presented in the pair of micrographs of matching fracture surfaces in Fig. 14. The arrows mark a local inhomogeneity in the structure which might have initiated fracture. Pull-outs this conspicuous were quite rare, but smaller ones would be difficult to identify in the general roughness of the fracture surface.

3.2.3. Weibull statistical analysis

The effect of gauge length on the tensile strength of a multifilament fibre with a predominance of surface flaws was determined for fibre E carbonized at 2100° C. The strength data, which show an inverse gauge length dependence, were analysed by using the two-parameter form of the Weibull equation of failure probability [6, 18]. The slopes of the Weibull plots shown in Fig. 15 indicate that a single mode of failure prevailed through the gauge length range. Fig. 16 presents a log–log plot of average strength versus gauge length based on the Weibull equation. The slope $(-1/m)$ of the line was determined by the average slope, m, of the plots in Fig. 15. Since a single population of flaws is indicated, the plot can be used to estimate the tensile strength at short gauge lengths, where values are difficult to measure experimentally. Extrapolation to a length of 0.3 mm, which is estimated as the approximate load transfer length in composites for multifilament fibre of this diameter [19], gives a tensile strength of approximately 3.8 GPa.

4. Discussion

The common sources of failure of the monofilaments were particles containing mineral elements or iron. Precautions to ensure cleanliness of the mesophase pitches have clearly improved the tensile strengths of the fibres. Carbon filaments from clean mesophase pitches were between 40% and 120% stronger than their contaminated counterparts measured at the same gauge length. The most common critical flaws in the contaminated fibres were ferrous particles introduced from stainless steel processing equipment.

A previous Weibull statistical analysis of tensile strengths of carbon monofilaments similar to clean fibre B resulted in a predicted strength of 5.3 GPa at 0.3 mm or 5.8 GPa at 0.2 mm, their estimated load transfer length in composites [6]. The present fractography study indicates that particles were very probably the principal flaws in the monofila-

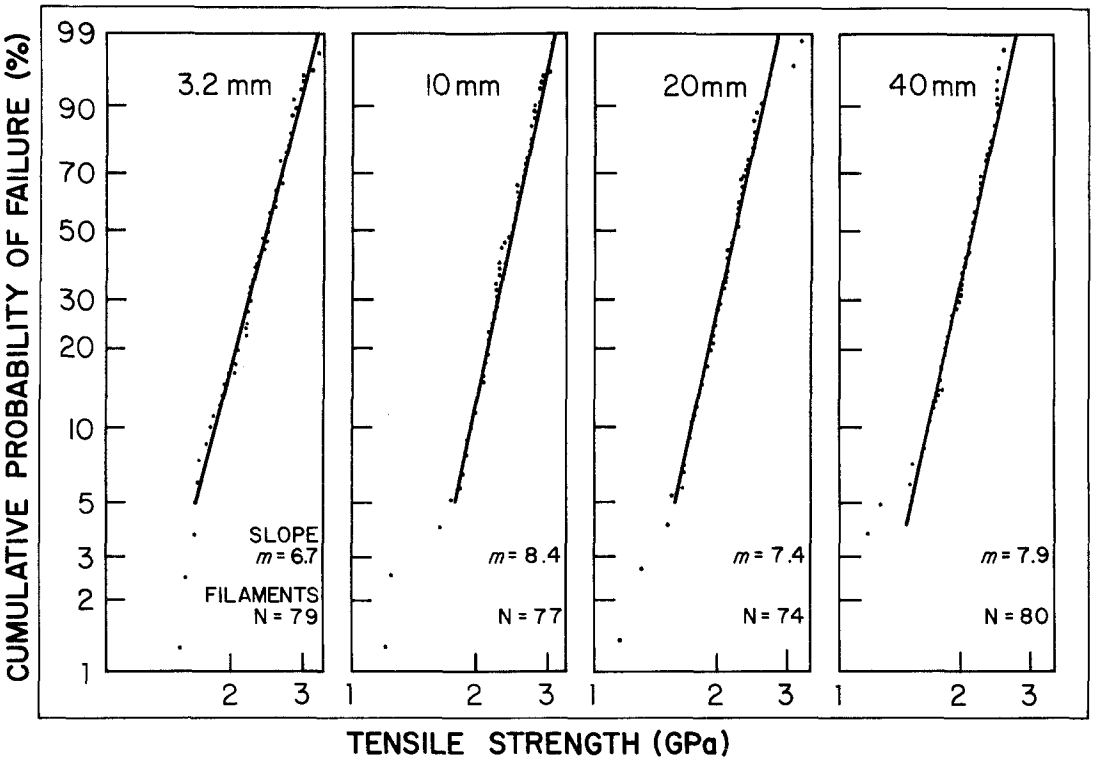

Figure 15 Weibull plots of strength distributions at various gauge lengths for filaments in fibre E carbonized at 2100° C. Average filament diameters at each gauge length are 10.7 μm with a standard deviation of 0.3 to 0.4.

ments at the gauge lengths used for strength extrapolation.

In the multifilaments, precautions to ensure cleanliness dramatically reduced both the size, and the frequency of appearance on fracture surfaces, of the particle flaws. At the same heat-treatment temperatures and gauge lengths, the clean multifilaments were between 40% and 70% stronger than the contaminated multifilaments. The contaminated multifilaments broke predominantly at mineral particles or at small surface holes that have been attributed to particles. A recognizable defect caused failure of every filament examined from fibre D. On the other hand, the clean multifilaments heated to 2100° C had so few particles on their fracture surfaces that their strengths were determined mostly by surface or undetected defects.

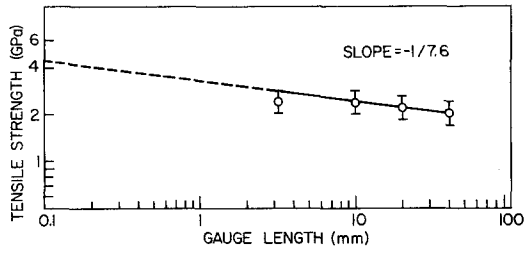

Figure 16 Tensile strength as a function of gauge length for fibre E carbonized at 2100° C. The bars show one standard deviation.

The deleterious effect of particle flaws on tensile strength was intensified by heating to high temperatures. Particles in fibres heated to 2500° C and above vaporized or reacted to form voids larger than the original inclusions, causing the tensile strengths of contaminated fibres to drop significantly. Since heating the clean fibre E to higher temperatures caused the voids from the tiny particles to enlarge while the surface defects were unaffected, particle flaws became more prominent on the fracture surfaces. The voids were much smaller than those in fibre D heated to corresponding temperatures, and the tensile strength of fibre E remained constant with heat-treatment temperature. Perhaps a slight decrease in strength caused by the flaw enlargement was counteracted by a slight increase in the intrinsic strength of the fibre upon heat treatment to higher temperatures.

Assuming that the undetected flaws in fibre E carbonized at 2100° C were isolated surface pits,

surface pitting was the predominant flaw in that batch. Surface defects in other carbon fibres have been reported by several investigators [9, 10, 12], and the origins of such flaws have remained obscure. The gauge length dependence of the strength of this batch was less (the value of m was greater) than it was for the monofilaments studied previously by Weibull analysis [6]. This low gauge length dependence indicates that pits were more uniformly distributed and closely spaced along the fibre than were the particle flaws in the monofilaments, a conclusion that is consistent with microscopy observations. Furthermore, in the multifilaments, the close spacing of the pits caused the strength extrapolated to 0.3 mm gauge length (3.8 GPa) to be less than that of the previous monofilaments (5.3 GPa), since, in the multifilaments, 0.3 mm is not a flaw-free length.

For both the present monofilaments and the multifilaments, a rough correlation can be drawn between the size of a defect and the stress at which the fibre broke. Defects of 3 μm in size or larger, anywhere in the filament cross-section, limited the strength to below 1.4 GPa. Interior flaws between 2 and 3 μm in size or surface flaws between 1 and 3 μm in size caused failure at strengths between 1.4 and 2.1 GPa. Surface or interior flaws between 0.7 and 2 μm in diameter or areas of extensive shallow pitting caused failure at strengths between 2.1 and 2.8 GPa. Fracture surfaces of fibres with strengths above 2.8 GPa contained particles or holes 1 μm or less in diameter, surface pits, or undetected defects. Fibres with strengths above 3.5 GPa failed at holes 0.5 μm or less in size, at shallow surface pits, or at undetected defects. The scatter associated with single-filament testing prevented quantification of the effect of flaw size in more detail.

5. Conclusions

(1) Improvement in tensile strengths of mesophase pitch-based carbon fibres can be achieved by ensuring that the pitch is kept clean during fibre preparation.

(2) The major flaws in more contaminated monofilament fibres were defects caused by stainless steel particles from processing equipment; those in the cleaner monofilaments were caused by stainless steel particles or mineral particles containing, for the most part, silicon and aluminium.

(3) The major flaws in the contaminated multifilaments were defects from mineral particles and smooth holes probably caused by particles of unknown composition.

(4) Particle voids enlarged at higher carbonization temperatures, causing an adverse effect on the tensile strengths of the contaminated multifilaments.

(5) The reduction of the size and frequency of particle flaws in the clean multifilaments allowed the strength to remain constant over a wide range of carbonization temperatures.

(6) Surface pits became the predominant critical flaw in the absence of particles.

References

1. R. MORETON, *Fibre Sci. Tech.* **1** (1969) 273.
2. R. MORETON, W. WATT and W. JOHNSON, *Nature* **213** (1967) 690.
3. D. J. THORNE, *ibid.* **248** (1974) 754.
4. *Idem*, Third Conference on Industrial Carbons and Graphite (Society of Chemical Industry, London, 1971) p. 463.
5. R. BACON and W. A. SCHALAMON, *Appl. Polym. Symp.* **9** (1969) 285.
6. S. CHWASTIAK, J. B. BARR and R. DIDCHENKO, *Carbon* **17** (1979) 49.
7. P. E. MCMAHON, *SAMPE Quarterly* **6** (1974) 7.
8. R. J. DIEFENDORF and E. TOKARSKY, *Polym. Eng. Sci.* **15** (1975) 150.
9. J. W. JOHNSON, *Appl. Polym. Symp.* **9** (1969) 229.
10. J. W. JOHNSON and D. J. THORNE, *Carbon* **7** (1969) 659.
11. J. V. SHARP and S. G. BURNAY, "Carbon Fibres: Their Composites and Applications" (Plastics Institute, London, 1971) p. 68.
12. J. V. SHARP, S. G. BURNAY, J. R. MATTHEWS and E. A. HARPER, "Carbon Fibres: Their Place in Modern Technology" (Plastics Institute, London, 1974), p. 25.
13. M. A. A. JORRO, W. R. LADNER and T. R. RANTELL, *Carbon* **14** (1976) 219.
14. W. WATT and W. JOHNSON, Third Conference on Industrial Carbons and Graphite (Society of Chemical Industry, London) 1971, p. 417.
15. R. MORETON and W. WATT, *Nature* **247** (1974) 360.
16. J. B. BARR, S. CHWASTIAK, R. DIDCHENKO, I. C. LEWIS, R. T. LEWIS and L. S. SINGER, *Appl. Polym. Symp.* **29** (1976) 161.
17. J. V. SHARP and S. G. BURNAY, "Carbon '72" (Bad Honnef, Deutsche Keramische Gesellschaft, 1972) p. 310.
18. E. Y. ROBINSON, University of California Report UCRL-50622 (March 1969), (NSA **23** 38919).
19. A. KELLY, "Strong Solids" (Clarendon Press, Oxford, 1973) p. 172.

Received 31 January and accepted 3 March 1980.